ISSN 2220-315X (online)

World Journal of *Experimental Medicine*

World J Exp Med 2016 November 20; 6(4): 63-79

Published by Baishideng Publishing Group Inc

WJEM World Journal of Experimental Medicine

A peer-reviewed, online, open-access journal of experimental medicine

Editorial Board

2016-2019

The *World Journal of Experimental Medicine* Editorial Board consists of 376 members, representing a team of worldwide experts in experimental medicine. They are from 43 countries, including Argentina (4), Australia (9), Belgium (4), Benin (1), Brazil (4), Canada (8), China (40), Croatia (2), Czech Republic (2), Denmark (1), Egypt (2), Finland (3), France (12), Germany (13), Greece (8), Hungary (1), India (14), Iran (1), Ireland (2), Israel (6), Italy (28), Japan (25), Kuwait (1), Lebanon (1), Malaysia (3), Mexico (4), Netherlands (5), Norway (2), Portugal (2), Rwanda (1), Saudi Arabia (4), Serbia (1), Singapore (2), Slovenia (2), South Korea (26), Spain (11), Sweden (7), Switzerland (2), Turkey (10), Ukraine (1), United Arab Emirates (1), United Kingdom (13), United States (87).

Javier Camacho, *Mexico City*
José F Munoz-Valle, *Zapopan*
Eduardo Pérez-Campos, *Oaxaca*

Netherlands

Reinoud Gosens, *Groningen*
Anya N Milne, *Utrecht*
Esmaeil Mortaz, *Utrecht*
Cornelis FM Sier, *Leiden*
Ruurd Torensma, *Nijmegen*

Norway

Kristian Gundersen, *Oslo*
Leiv Ose, *Oslo*

Portugal

Fatima Baltazar, *Braga*
Fani Sousa, *Covilhã*

Rwanda

Wondatir Nigatu, *Kigali*

Saudi Arabia

Jaffar A Al-Tawfiq, *Dhahran*
Giovanni Di Salvo, *Riyadh*
Volodymyr Dvornyk, *Riyadh*
Mostafa M El-Naggar, *Jazan*

Serbia

Lidija Radenovic, *Belgrade*

Singapore

Madhav Bhatia, Singapore
Ivy Ho, *Singapore*

Slovenia

Damjan Glavac, *Ljubljana*
Srdjan Novaković, *Ljubljana*

South Korea

Dal-Woong Choi, *Seoul*
Kang-Yell Choi, *Seoul*
Sangdun Choi, *Suwon*
Young-Hwa Chung, *Busan*
Joohun Ha, *Seoul*
Kwon-Soo Ha, *Chuncheon*
Eui-Bae Jeung, *Cheongju*
Eun-Jung Jin, *Jeonbuk*
Chang-Duk Jun, *Gwangju*
Min Hyung Jung, *Seoul*
Sung-Chul Jung, *Seoul*
Young Do Jung, *Kwangju*
Hyung-Ryong Kim, *Chonbuk*
Jae Ho Kim, *Yangsan*
Jung Mogg Kim, *Seoul*
Kyu-Won Kim, *Seoul*
Se-Kwon Kim, *Busan*
Jong-Young Kwak, *Pusan*
Jeung-Hoon Lee, *Daejeon*
Jung Weon Lee, *Seoul*
Seong-Wook Lee, *Yongin*
Soo Young Lee, *Seoul*
Do Sik Min, *Pusan*
Yunbae Pak, *Jinju*
Baik Lin Seong, *Seoul*
Soon Young Shin, *Seoul*

Spain

Salvador F Alino, *Valencia*
Isabel Andia, Zamudio *Vizcaya*
Jaime Arias, *Madrid*
Javier Arias-Diaz, *Madrid*
Vicente Felipo, *Valencia*
Navarra JA Martínez, *Pamplona*
Miguel ángel Medina, *Malaga*
Jose A Obeso, *Pamplona*
Jose Prados, *Granada*
Osta P Rosario, *Zaragoza*
Jose C Segovia, *Madrid*

Sweden

Karl O Fagerstrom, *Helsingborg*
Robert Hahn, *Sodertalje*
Susanne Jacobsson, *Örebro*
Stefan Karlsson, *Lund*
Marek J Los, *Linkoping*
Jin-Jing Pei, *Tumba*
Xiao-Feng Sun, *Linkoping*

Switzerland

Florian Bihl, *Bellinzona*
Witold Kilarski, *Lausanne*

Turkey

Ali K Adiloglu, *Ankara*
Mutay Aslan, *Antalya*
Hakan Erdem, *Ankara*
Semin M Fenkci, *Denizli*
Askin Hekimoglu, *Diyarbakir*
Suleyman S Koca, *Elazig*
Cuneyt Narin, *Konya*
Mustafa Taskesen, *Diyarbakir*
Mehmet Tokac, *Konya*
Selma Yilmazer, *Istanbul*

Ukraine

Tamara M Kuchmerovska, *Kyiv*

United Arab Emirates

Azzam A Maghazachi, *Sharjah*

United Kingdom

Charles W Archer, *Cardiff*
Dominique Bonnet, *London*
Neil Davie, *Kent*
David Gilham, *Manchester*
Paul Hamilton, *Belfast*
Simon Langdon, *Edinburgh*
Tarik Massoud, *Cambridge*
Dipak P Ramji, *Cardiff*
Cordula M Stover, *Leicester*
Olga Tura, *Edinburgh*
Mark Wareing, *Manchester*
Adam Wright, *Liverpool*
Shi-Yu Yang, *London*

United States

Anshu Agrawal, *Irvine*
Arshak R Alexanian, *Milwaukee*
Mikhail Alexeyev, *Mobile*
Robert J Amato, *Houston*
Ragheb A Assaly, *Toledo*
Laure Aurelian, *Baltimore*
Joseph M Backer, *Brookfield*
Raymond T Bartus, *San Diego*
Ajay S Behl, *Minneapolis*
Fabian Benencia, *Athens*
Arun Bhunia, *West Lafayette*
Ramireddy Bommireddy, *Tucson*
Michael Borchers, *Cincinnati*
Alexander A Bukreyev, *Galveston*
Carlos Caulin, *Houston*
Arvind Chhabra, *Farmington*
Maurizio Chiriva, *Lubbock*
Yingzi Cong, *Galveston*
Akram Da'darah, *North Grafton*
Guillaume Darrasse-Jèze, *New York*
Murat Digicaylioglu, *San Antonio*
Liu-Tao Du, *Los Angeles*
Nejat Düzgüne, *San Francisco*
Charles E Egwuagu, *Bethesda*
Lian-Chun Fan, *Indianapolis*
Bing-Liang Fang, *Houston*
Markus H Frank, *Boston*
Pramod K Giri, *Athens*
Zong-Sheng Guo, *Pittsburgh*
Diane M Harper, *Louisville*
Mohamed Hassan, *Jackson*
Kremer Heidemarie, *Miami*
Marta Herreros-Villanueva, *Rochester*
Cory M Hogaboam, *Ann Arbor*
Ji-Fan Hu, *Palo Atlo*

World Journal of Experimental Medicine

Contents

Quarterly Volume 6 Number 4 November 20, 2016

ORIGINAL ARTICLE

Basic Study

World Journal of Experimental Medicine
Volume 6 Number 4 November 20, 2016

Contents

NAME OF JOURNAL
World Journal of Experimental Medicine

ISSN
ISSN 2220-315X (online)

LAUNCH DATE
December 20, 2011

FREQUENCY
Quarterly

EDITORIAL OFFICE
Xiu-Xia Song, Director
Fang-Fang Ji, Vice Director
World Journal of Experimental Medicine
Baishideng Publishing Group Inc
8226 Regency Drive, Pleasanton, CA 94588, USA
Telephone: +1-925-2238242
Fax: +1-925-2238243
E-mail: editorialoffice@wjgnet.com
Help Desk: http://www.wjgnet.com/esps/helpdesk.aspx
http://www.wjgnet.com

PUBLISHER
Baishideng Publishing Group Inc
8226 Regency Drive,
Pleasanton, CA 94588, USA
Telephone: +1-925-2238242
Fax: +1-925-2238243
E-mail: bpgoffice@wjgnet.com
Help Desk: http://www.wjgnet.com/esps/helpdesk.aspx
http://www.wjgnet.com

PUBLICATION DATE
November 20, 2016

INSTRUCTIONS TO AUTHORS
http://www.wjgnet.com/bpg/gerinfo/204

ONLINE SUBMISSION
http://www.wjgnet.com/esps/

World Journal of Experimental Medicine

Submit a Manuscript: http://www.wjgnet.com/esps/
Help Desk: http://www.wjgnet.com/esps/helpdesk.aspx
DOI: 10.5493/wjem.v6.i4.63

World J Exp Med 2016 November 20; 6(4): 63-71
ISSN 2220-315X (online)

ORIGINAL ARTICLE

Basic Study

Lipofuscins prepared by modification of photoreceptor cells *via* glycation or lipid peroxidation show the similar phototoxicity

Alexander Dontsov, Anna Koromyslova, Mikhail Ostrovsky, Natalia Sakina

Alexander Dontsov, Anna Koromyslova, Mikhail Ostrovsky, Natalia Sakina, Emanuel Institute of Biochemical Physics, Russian Academy of Sciences, 119334 Moscow, Russia

Author contributions: All authors contributed to this manuscript.

Supported by The Russian Foundation for Basic Research, No. 15-29-03831.

Institutional review board statement: The study reviewed and approved by the Emanuel Institute of Biochemical Physics.

Institutional animal care and use committee statement: The study reviewed and approved by the Emanuel Institute of Biochemical Physics. Animals subjects were not involved in our experimental study.

Conflict-of-interest statement: The authors have no conflict of interest.

Data sharing statement: No additional data are available.

Manuscript source: Invited manuscript

Correspondence to: Natalia Sakina, PhD, Senior Researcher, Emanuel Institute of Biochemical Physics, Russian Academy of Sciences, Kosygina st. 4, 119334 Moscow, Russia. nsakina@mail.ru
Telephone: +7-495-9397422
Fax: +7-499-1374101

Received: June 29, 2016
Peer-review started: July 1, 2016
First decision: September 5, 2016
Revised: September 19, 2016
Accepted: October 17, 2016
Article in press: October 19, 2016
Published online: November 20, 2016

Abstract

AIM

To investigate the effect of two ways of lipofuscin production (lipid peroxidation and glycation) on lipofuscin fluorescence characteristics and phototoxicity and to compare them with the properties of natural lipofuscin.

METHODS

Model lipofuscins were prepared on the basis of bovine photoreceptor outer segments (POS) with bisretinoid A2E addition. One set of samples was prepared from POS modified by lipid peroxidation, while another set from POS modified by glycation with fructose. Fluorescent properties and kinetics of photoinduced superoxide generation of model lipofuscins and human retinal pigment epithelium (RPE) lipofuscin were compared. The fluorescence spectra of samples were measured at 365 nm excitation wavelength and 380-650 emission wavelength.

RESULTS

The fluorescence spectra of model lipofuscins are almost the same as the spectrum of natural lipofuscin. Visible light irradiation of both model lipofuscins and natural lipofuscin isolated from RPE cells leads to decrease of a fluorescence maximum at 550 nm and to appearance of a distinct, new maximum at 445-460 nm. The rate of photogeneration of reactive oxygen forms by both model lipofuscins was almost the same and approximately two times less than that of RPE lipofuscin granules.

CONCLUSION
These data suggest that fluorescent characteristics and phototoxicity of lipofuscin granules depend only to an insignificant degree on the oxidative modification of POS proteins and lipids, and generally are defined by the bisretinoid fluorophores contained in them.

Key words: Model lipofuscins; Retinal pigment epithelium; Photoreceptor outer segments; Bisretinoids; Glycation; Lipid peroxidation; Superoxide

Core tip: The aim of this work is to investigate the influence of different ways of protein-lipid modification of photoreceptor outer segments (POS) on the spectral characteristics and toxicity of lipofuscin. Therefore, model lipofuscins were prepared by protein-lipid modification of POS with products of lipid peroxidation or glycation reaction and the subsequent addition of the fluorophore A2E. The type of photoreceptor modification has no effect on model lipofuscins phototoxicity.

Dontsov A, Koromyslova A, Ostrovsky M, Sakina N. Lipofuscins prepared by modification of photoreceptor cells *via* glycation or lipid peroxidation show the similar phototoxicity. *World J Exp Med* 2016; 6(4): 63-71 Available from: URL: http://www.wjgnet.com/2220-315X/full/v6/i4/63.htm DOI: http://dx.doi.org/10.5493/wjem.v6.i4.63

INTRODUCTION

Fluorescent (aging pigment) lipofuscin accumulates during lifetime and is one of the most important factors limiting the life of a cell. Lipofuscin is found in tissues of various organs such as brain, heart, liver, kidneys and skin. Especially a lot of lipofuscin accumulates in aging postmitotic tissues such as nerve and muscle. Lipofuscin is insoluble and cannot to be utilized by neither lysosomal enzymes nor proteasomal system of a cell[1].

In the eye lipofuscin is largely accumulated in the retinal pigment epithelium cells (RPE)[2], being one of the key biomarkers of aging and oxidative stress. It also plays an important role in the development of retinal pathologies[3].

RPE lipofuscin granules are composed of a complex mixture of fluorophores, which determine fluorescent characteristics of a granule[4]. The most studied fluorophore of lipofuscin granules is pyridinium bisretinoid - A2E[5].

Both lipofuscin granules and fluorophore A2E are toxic to cells. Upon irradiation with visible light, they are able to generate reactive oxygen species[6-8], enforce damage of membrane structures[9-11], inhibit lysosomal and proteasome degradation of proteins[12-14] and lipids[15], as well as to induce apoptosis of RPE cells[16,17].

It is generally accepted that lipofuscin granules are formed as a result of incomplete digestion during phagocytosis of exhaust disks of photoreceptor outer segments (POS) in RPE cells. Inability of proteins and lipids in lipofuscin granules to be utilized is associated with the processes of oxidation and formation of intra- and inter-molecular covalent cross-linking. This modification of molecules in granules is considered to be mainly connected to reactions of lipid peroxidation that can actively pass in the retina and RPE tissues[18]. The reactive electrophilic aldehydes produced by process of lipid peroxidation, especially malondialdehyde (MDA) and 4-hydroxynonenal (4-HNE), react readily with amino acid residues of lysine, histidine, cysteine and arginine, as well as with amino groups of phospholipids. This results in damage and disruption of their structure and catabolism[19]. Indeed, most of the proteins identified in lipofuscin from human RPE are modified in reactions with MDA and 4-HNE[19]. Proteins modified by lipid peroxidation reactions are called advanced lipoxidation end products (ALE).

Reduced susceptibility of phagolysosome proteins to proteolysis after their modification by malondialdehyde and 4-hydroxynonenal is supposed to be an important factor in lipofuscinogenesis[20].

However, it is well known that covalently crosslinked proteins and lipids are also produced under conditions of hyperglycaemia resulting from the Maillard reaction[21]. These so-called advanced glycation end products (AGE) are believed to play an important role in the development of diabetic complications[22] and various eye pathologies[23]. AGE products were found to accumulate with age in cadaver eyes within the RPE in Bruch's membrane and drusen[24,25]. AGE accumulation leads to the reduced activity of lysosomal enzymes and, consequently, to the increased accumulation of lipofuscin[25].

AGE products were also found directly in lipofuscin granules. Horie *et al*[26] has first shown that lipofuscin from brain tissue of elderly people is formed not only in reactions of lipid peroxidation, but also in glycation reactions. Apparently, this can also occur in the lipofuscin granules of the RPE. For instance, AGE-modified proteins were also found in lipofuscin granules of human RPE[19].

All in all, that suggests that during lipofuscinogenesis modification of proteins and lipids in phagolysosome of RPE cells can occur either as a result of lipid peroxidation and ALE products formation, or by glycation reactions and formation of AGE products. The later can happen if there is an increased content of reducing sugars in the cell. There is currently no information about the properties of lipofuscin granules formed under the conditions of hyperglycemia. The aim of this work is to investigate the influence of different ways of protein-lipid modification on the spectral characteristics and toxicity of lipofuscin. It is assumed that the fluorescence of RPE lipofuscin determines the fundus autofluorescence (FAF) *in vivo*[27,28]. Monitoring FAF is noninvasive diagnostic method used in detection retinal degenerative diseases such as recessive

Stargardt disease, Best macular dystrophy, age-related macular degeneration (AMD) and Diabetic Retinopaty[3]. So the model systems of lipofuscin study may be important for FAF interpretation. Therefore, model lipofuscin was prepared on the basis of POS and the fluorophore A2E. Model lipofuscin preparing was accomplished by corporating modified POS and the fluorophore A2E. Modification of POS was carried out either by the reaction with products of lipid peroxidation (LPO-lipofuscin model), or by glycation reaction in the presence of fructose (LFF-lipofuscin model). Properties of the model lipofuscins were compared with natural lipofuscin from human eye RPE.

MATERIALS AND METHODS

Isolation of lipofuscin granules from human RPE

Cadaver eyes from 40-75 years old donors without any ophthalmic diseases were kindly provided by the Eye Tissue Bank of the Sv. Fyodorov Eye Microsurgery Institute, Moscow. Experiments on tissue isolated from human-cadaver eyes were performed in compliance with officially accepted procedures, in particular Russian Federation law N 4180-I dated 22.12.1992, "on human organs or tissue transplantation" (with modifications and additions dated 20.06.2000, 16.10.2006, 09.02.2007, and 29.11.2007); section Ⅱ "removal of organs or tissue from dead bodies"; clause 8 "presumption of consent for removal of organs or tissue"; clause 10 "permission to remove organs or tissue from dead bodies". According to section Ⅱ (clause 8) of this law, consent from the donor or the next of kin to use organs or tissue is not required[29]. On the basis of the Russian Federal Service on Surveillance in Healthcare (Roszdravnadzor) licenses No. 99-01-005317 dated 30.04.2008 and No. FS-99-01-008251 dated 18.02.2013, the Eye Tissue Bank located in the Sv. Fyodorov Eye Microsurgery Complex (Beskudnikovsky bld. 59a, Moscow, Russia, 127486, http://www.mntk.ru/mntk-moscow/Scientific-units/biology/glaznoy_bank/) obtains human cadaver eyes from the mortuary departments of the Moscow Forensic Medical Examination Bureau. These licenses permit the use of tissue isolated from human-cadaver eyes for transplantation and scientific research. Permission was obtained from the chief medical officer of the Sv. Fyodorov Eye Microsurgery Complex, under a scientific collaboration agreement between the Complex and the Emanuel Institute of Biochemical Physics dated 11.01.2011, to perform scientific research in the Laboratory of Physical and Chemical Bases of Vision at the Institute with RPE from cadaver eyes. Cadaver eyes, after removal of corneas for transplantation, were delivered by the Eye Tissue Bank to the Laboratory by road in a box for human organs. Cadaver eyes after isolation of RPE were returned to the Eye Tissue Bank for use, in compliance with officially accepted procedures.

Lipofuscin granules were isolated from RPE cells by a modified technique described in[30]. The obtained granules were dissolved in phosphate buffer and stored at -70 ℃.

Isolation of POS

POS were isolated from bovine retinas by a modified method of McDowell[31]. Obtained POS were dissolved in 0.1 mol/L potassium phosphate buffer (pH 7.6) and stored at -20 ℃.

A2E chemical synthesis

A2E samples were synthesized and purified by the method described in[32]. Briefly, a mixture of all-trans-retinal and ethanolamine (Sigma) in a ratio of 2.3:1 in absolute ethanol was stirred in the presence of acetic acid (1 eq.) at room temperature in the dark for 2.5 d. The mixture was then evaporated under vacuum; the pellet was dissolved in chloroform (Himmed, Russia) and chromatographed on a silica gel-chloroform column (200-400 mesh, 60 A, Sigma). Purified A2E was dissolved in methanol (Sigma). Purity of final A2E was monitored by HPLC on a chromatograph Knauer (Germany), fitted with a Diasfer-110 C18 reverse phase analytical column, and with the mobile phase consisting of acetonitrile/water (84% of acetonitrile in mobile phase) + 0.1% trifluoroacetic acid (TFA)[33].

Preparation of model lipofuscins

The model lipofuscins were prepared from POS[34].

Model of lipofuscin from oxidized POS: POS from bovine eyes were subjected to the process of autoxidation. A suspension of POS containing 10-12 mg protein per 1 mL K-phosphate buffer was incubated at 4 ℃ in the dark for 30-45 d. The concentration of TBA-reactive substances in the autooxidised POS was 12.0 ± 1.0 nmol/mg protein. Autooxidised POS were dissolved in 0.1 mol/L K-phosphate buffer, pH 7.6 (final concentration 1.3-1.5 mg protein/mL) and incubated at 37 ℃ in the dark with constant stirring for 72 h. After incubation, modified POS were dialyzed against phosphate buffer to remove unreacted low molecular weight molecules. For dialysis, Float-A-Lyser (SPECTRUM Labs) cellulose-ester membranes with a Molecular Weight Cut-Off of approximately 3.5 kDa were used. Dialysis was carried out for 1.5 d at 6 ℃. Solution of the A2E in methanol was added to the purified modified POS to a final concentration of 60-70 nmol/mL. The prepared complex was centrifuged at 10000 g in a Beckman Allegra 64R centrifuge for 20 min. The pellet was resuspended in 0.1 mol/L K-phosphate buffer (LFO-lipofuscin).

Model lipofuscin from weakly oxidized POS: Freshly prepared POS from bovine eyes (concentration of TBA-reactive substances did not exceed 0.5-0.7 nmol/mg protein) were dissolved in 0.1 mol/L K-phosphate buffer containing 50 mmol/L fructose (Sigma), to a final concentration of 1.3-1.5 mg protein/mL and incubated with constant stirring at 37 ℃ for 72 h in the dark. No fructose was added to the control samples. After incubation, modified samples were treated in the same way as oxidized POS. The final pellet was resuspended in 0.1 mol/L K-phosphate buffer (LFF-lipofuscin).

Determination of wet weight of lipofuscin

To determine the wet weight of natural and model lipofuscin aliquots of samples were subjected to centrifugation using Amicon-Ultra-0.5 filters at 10000 g for 30 min. The concentration of samples was calculated in mg wet weight per 1 mL. For our samples it was the following: LFO-lipofuscin approximately 110 ± 15 mg/mL, LFF-lipofuscin approximately 80 ± 12 mg/mL and for RPE lipofuscin approximately 100 ± 20 mg/mL. A2E content in model lipofuscins was approximately 0.8-1.0 nmol/mg of wet weight. A2E concentration was calculated by using $\varepsilon = 3.1 \times 10^4$/mol/L per centimeter at 430 nm wavelength.

The fluorescence spectra

The fluorescence spectra of samples were measured on a spectrofluorometer (Shimadzu RF-5301) at 365 nm excitation wavelength and 380-650 emission wavelength. All experiments were made using pure solvent as a reference.

Irradiation of samples

For irradiation of samples an incandescent lamp KGM 24-150, 150 watt, equipped with a focusing system and heat filter was used. Irradiation energy was 80 mW/cm^2. Illumination was carried out under constant stirring at room temperature, monitoring the initial sample volume. The spectral range of irradiation was set to 390-700 nm.

Concentration of peroxidation products

The concentration of peroxidation products was determined by the accumulation of the reaction products with thiobarbituric acid (Sigma) (TBA-reactive substances - TBARS), which was measured by absorption at a wavelength of 532 nm[35].

The concentration of superoxide radicals

The superoxide concentration was measured by cytochrome c reduction (Fe^{3+}), inhibited by superoxide dismutase by a modified method from[36]. The reaction mixture contained Hanks buffer supplemented with 20 mmol/L sodium bicarbonate, pH 7.6, 100 mmol/L cytochrome c, 50 μg/mL catalase and 0.05% cetyltrimethylammonium bromide. The concentration of model lipofuscins and lipofuscin from human RPE in the samples was 3-5 mg/mL. All reagents used for this method were obtained from Sigma. The mixture was irradiated with visible light (irradiation energy 80 mW/cm^2) under constant stirring. Superoxide concentration was measured in a spectrophotometer (Shimadzu UV-1700) by the increase in maximum absorbance at 550 nm (molar absorption 21/mol/L per centimeter)[37].

Statistical analysis

The data were expressed as the mean ± SD. For the statistics, Student's *t*-test was used. $P < 0.05$ was considered as statistically significant.

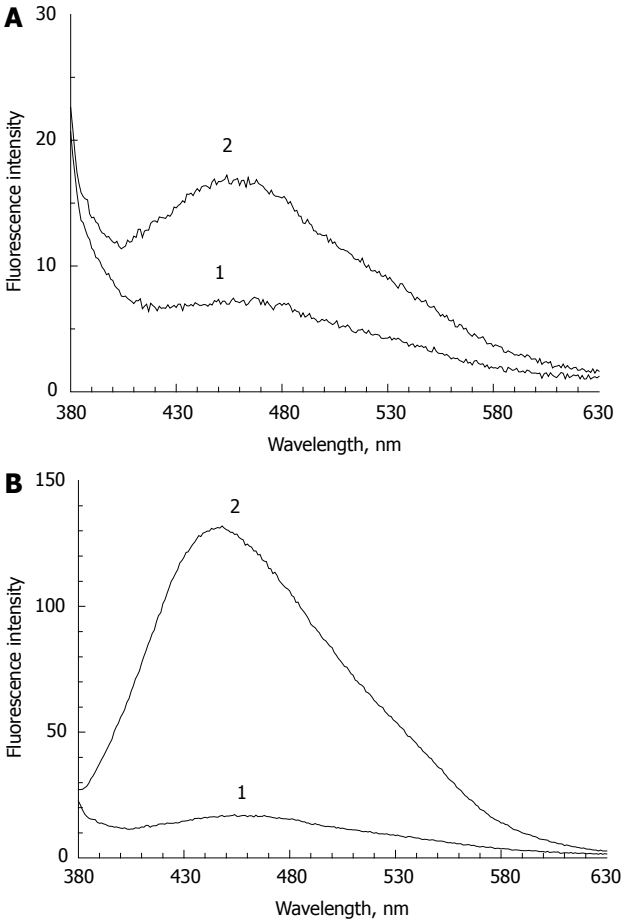

Figure 1 Fluorescent products accumulation in weakly oxidised bovine photoreceptor outer segments after 72 h incubation at 37 ℃. A: POS fluorescence incubated in the absence of fructose: curve 1 - prior to incubation; curve 2 - after incubation; B: POS fluorescence incubated in the presence of fructose: curve 1 - prior to incubation; curve 2 - after incubation. Fluorescence was measured in 0.1 mol/L K-phosphate buffer, pH 7.6, excitation wavelength - 365 nm.

RESULTS

Model lipofuscin fluorescence spectra are not altered by the ways of POS modifications

The preparation of model lipofuscin samples included two stages. First stage - modification of proteins and lipids from POS during incubation at 37 ℃ in the presence of either lipid autoxidation products (oxidation way) or fructose (glycation way).

Figure 1 shows the fluorescence spectrum of POS samples containing a small concentration of peroxidation products and incubated in the absence (Figure 1A) or presence (Figure 1B) of fructose. In the absence of fructose, a 72-h incubation causes an approximately two-fold increase in the fluorescence maximum. In the presence of fructose, the intensity of POS fluorescence at 445-450 nm increased about 8 times. At the same time, an increase of absorption at a wavelength of 320 nm was observed (data not shown). It appears that optical absorption and fluorescence increases due to the glycation reaction and formation of fluorescent Schiff

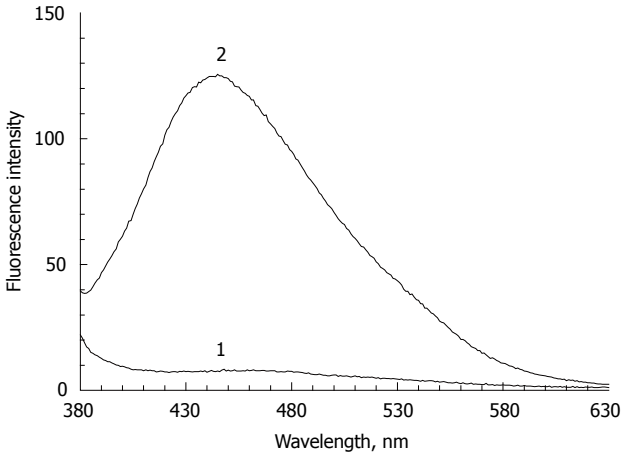

Figure 2 Fluorescent products accumulation in the pre-oxidized photoreceptor outer segments at 72 h incubation at 37 ℃. Curve 1 - prior to incubation; curve 2 - after incubation. Measurement conditions as in the legend under Figure 1.

bases in proteins and lipids. In the absence of sugar, this process is very slow and could be explained by residual products of lipid peroxidation.

In addition, following the incubation of POS samples with a high concentration of lipid peroxidation products, a significant increase in fluorescence intensity occurs (almost 15 times) irrespective of the fructose presence (Figure 2). In this case, the emission wavelength maximum practically coincides with the emission wavelength maximum of POS samples incubated with fructose.

The second stage of model lipofuscin preparation involves mixing modified and dialyzed POS with A2E followed by precipitation of the complex and solubilization of the precipitate in phosphate buffer, as described in Materials and Methods. This procedure leads to a significant change in spectral fluorescent characteristics of the modified POS. There was a significant decrease in fluorescence intensity at a wavelength of 445-450 nm (the major fluorescence peak observed before the addition of A2E, Figure 3A, curve 1) and an appearance of the emission maximum at 550 nm (Figure 3A, curve 2). The fluorescence maximum at 550 nm is typical for A2E and could be explained by the presence of these molecules in the model lipofuscin samples.

The reason for the sharp decrease of the fluorescence maximum at 445-450 nm is not fully understood. It could be due to fluorescence quenching of Schiff bases by A2E molecules or by their destruction.

Our model lipofuscins and lipofuscin from human RPE have very similar fluorescence spectra. Figure 3B shows the fluorescence spectra of LFO lipofuscin (curve 1) and natural lipofuscin (dashed curve 2) at an excitation wavelength of 365 nm. The spectra are almost completely identical. It should be appreciated, however, that the fluorescence emission spectra of lipofuscin from human RPE can considerably vary at excitation 360-365 nm, producing emission maxima between 460 and 630 nm[38].

This dispersion appears to depend on many factors,

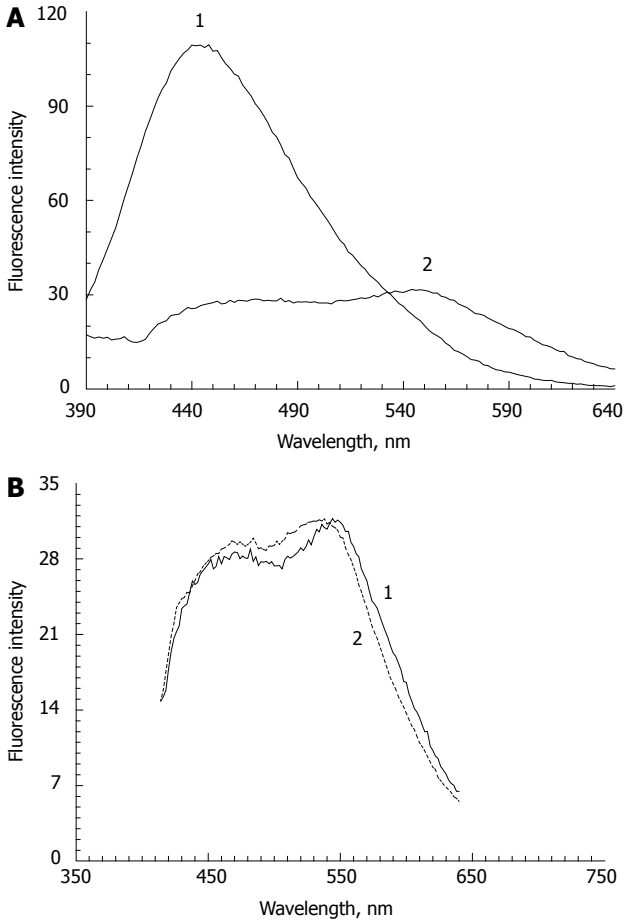

Figure 3 Production of model lipofuscin in the reaction between modified photoreceptor outer segments and bisretinoid A2E. A: A2E binding by modified photoreceptor outer segments leads to a change in their fluorescence characteristics: curve 1 - POS modified oxidized prior to incubation with A2E; curve 2 - modified POS containing A2E (LPO - lipofuscin); B: Comparison of fluorescence characteristics of the model lipofuscin (LPO) and natural lipofuscin granules from human RPE: curve 1 (solid line) - LPO; curve 2 (dotted line) - lipofuscin granules from human RPE. Model lipofuscin preparation is described in materials and methods, excitation wavelength - 365 nm. POS: Photoreceptor outer segments; RPE: Retinal pigment epithelium.

including age and diet quality[39]. The fluorescence spectra of the LFO and LFF lipofuscins in these conditions were almost identical. These results show that the fluorescence spectrum of the lipofuscin model is largely determined by its fluorophores content; in this case, the fluorophore A2E.

The photobleaching processes of both model and RPE lipofuscins demonstrate very similar kinetics

Figure 4 shows the fluorescence spectra of LFF lipofuscin (Figure 4A) and lipofuscin from RPE (Figure 4B) upon irradiation with visible light with different exposures. It can be seen that in both cases the 550 nm peak disappears while the fluorescence amplitude significantly increases in the short wavelength region. Emission maximum after a 3-h exposure is shifted to 445-450 nm for LFF and to 460 nm for RPE lipofuscin. Apparently, the reason for this shift is associated with

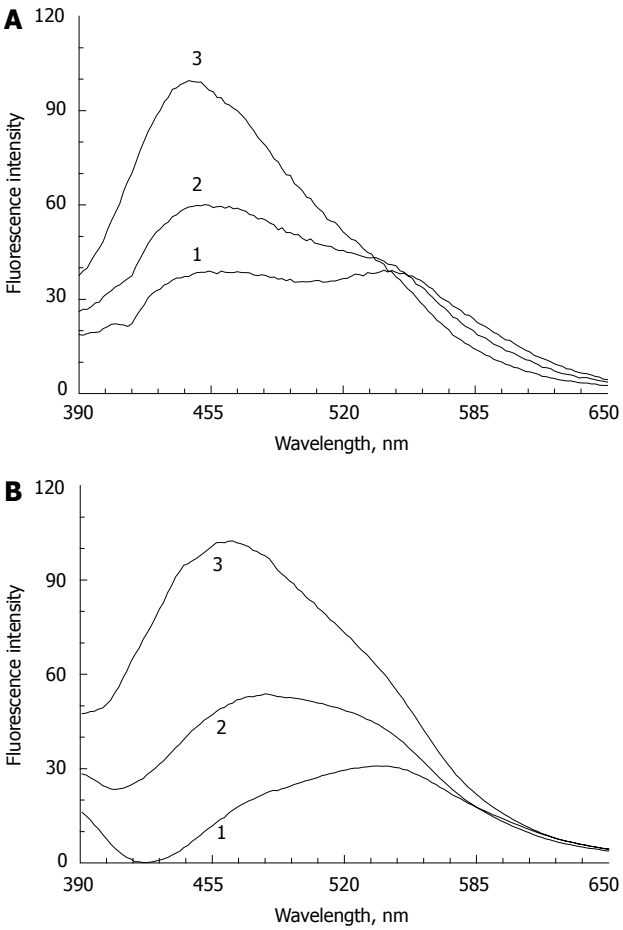

Figure 4 Effect of visible light irradiation on the fluorescence characteristics of lipofuscin. A: Change of fluorescence spectra of the model lipofuscin (LFF): 1 - prior to irradiation, 2 and 3 - after irradiation for 1 and 3 h, respectively; B: Change of fluorescence spectra of human RPE lipofuscin granules: 1 - prior to irradiation, 2 and 3 - after irradiation for 1 and 3 h, respectively. RPE: Retinal pigment epithelium.

photodestruction of fluorophore A2E, leading to the formation of its oxidized derivatives[4]. The fluorescence spectra of these oxidized compounds are shifted to a shorter wavelength range.

It is also possible that A2E destruction reveals the underlying fluorescence of modified POS proteins and lipids. Because the model lipofuscin contains only fluorophore A2E, but RPE lipofuscin contains a mixture of different fluorophores, we can assume that, in natural RPE lipofuscin fluorophore A2E plays an important role in determining the total fluorescence.

Irradiation of model lipofuscins show almost the same rate of superoxide photogeneration

Lipofuscin phototoxicity is known to be primarily determined by the ability of lipofuscin to generate reactive oxygen species. We have previously shown that phototoxicity of RPE lipofuscin is higher than toxicity of just its A2E content[11]. This is probably due to the presence of other more active fluorophores in lipofuscin granules.

Model lipofuscins, prepared in this study, contain only one fluorophore A2E. Figure 5 shows the comparative

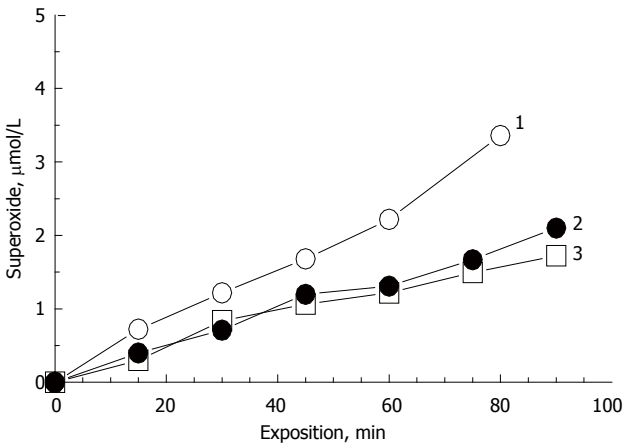

Figure 5 Comparative kinetics of superoxide generation by irradiation of natural lipofuscin (curve 1) and model of lipofuscin (curve 2 - LFF, curve 3 - LPO). The reaction conditions - see methods. Lipofuscin concentrations - 2.5 mg/mL.

kinetics of photogenerated superoxide upon irradiation of model and RPE lipofuscins. Model lipofuscins contained about 0.8-1.0 nmol A2E per 1 mg wet weight of sample.

Irradiation of LFO and LFF lipofuscin samples exhibited almost the same rate of superoxide generation (curves 2 and 3). A2E content in RPE lipofuscin can be roughly estimated according to the data from[40]. In this study quantitative analysis of bisretinoids in human RPE lipofuscin showed that the average content of A2E and iso-A2E is 380 pmol per 5.5×10^7 lipofuscin granules, which corresponds to 6.4×10^{-18} mol/granule. The weight of one lipofuscin granule is 1.3 ± 0.2 pg[41], which gives the value of about 5 nmol/mg of A2E content in human RPE lipofuscin granules. This roughly corresponds to the A2E content in our model lipofuscin, assuming that the dry weight of the model pellets is about 20% of wet weight.

However, the rate of superoxide photogeneration catalyzed by RPE lipofuscin (curve 1, Figure 5) was significantly higher compared to that of model lipofuscin (curves 2 and 3, Figure 5). Average rates of superoxide photogeneration in all experiments are presented in the Table 1. The higher rate of superoxide photogeneration by RPE lipofuscin compared to A2E-containig model lipofuscins could be explained by the presence of other photoactive fluorophores[11,42-44] because the concentration of A2E in RPE lipofuscin does not exceed the concentration of the fluorophore in the model lipofuscins.

DISCUSSION

As noted earlier, lipid peroxidation products are undoubtedly important for the formation of lipofuscin. Although the process of AGE products accumulation during normal aging has been well studied, much less is known about the role of advanced glycation end products in the formation of lipofuscin, which accumulates with age in RPE cells[45].

An important role in this process belongs to fructose.

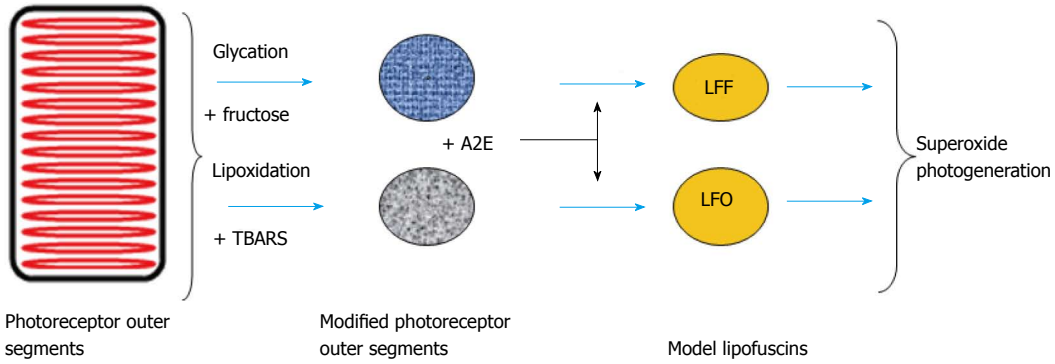

Figure 6 Schema of processes generation of retinal pigment epithelium lipofuscin from modified photoreceptor outer segments and fluorophore A2E. POS: Photoreceptor outer segments; TBARS: TBA-reactive substances.

Table 1 Superoxide generation rate in model and natural lipofuscins

Sample name	Superoxide generation rate nmole/min mg wet weight
Model lipofuscin from oxidized POS (LPO-lipofuscin)	8.5 ± 0.6
Model lipofuscin obtained from not oxidized POS in the presence of fructose (LFF-lipofuscin)	9.2 ± 0.4
Natural lipofuscin from human eye	15.7 ± 0.8

Data represents mean values of 5 measurements on each type of lipofuscin with standard deviation, $P < 0.05$. POS: Photoreceptor outer segments.

Although its concentration in the blood is significantly lower than the glucose concentration (approximately 35 μmol/L, while the concentration of glucose is approximately 5 mmol/L), the cellular concentration of fructose can be much higher. This increase could be induced by hyperglycaemic conditions when fructose formation through the polyol pathway is activated[46]. An elevated concentration of glucose is known to activate the cellular enzyme aldose reductase, which catalyzes the transformation of glucose into sorbitol. Sorbitol is then oxidized to fructose in a reaction catalyzed by the polyol dehydrogenase enzyme. It has been established that the retina and RPE are characterized by high expression of aldose reductase under hyperglycaemia[47-49].

Fructose is a much more effective glycation agent in Maillard reactions than glucose. This is probably due to the fact that the open form of glucose molecules, which is directly involved in the Maillard reaction, is present at only 0.0002% of the content of the inactive cyclic form, whereas the fructose open form reaches 0.7% of the cyclized form[50]. A significant difference between glucose and fructose in the induction of carbonylation of target molecules may be explained by the formation of glyceraldehyde during fructose metabolism, while during glucose metabolism glyceraldehyde-3-phosphate is formed, which is much less active in Maillard reactions[51].

Hyperglycaemia and polyol path activation greatly increase retinal sensitivity to oxidative stress[52]. All these facts suggest that aging and diabetes create conditions in the retina and in RPE cells that promote development of advanced glycation reactions. Therefore, in lipofuscin, cross-links in proteins and lipids may form, not only by their interaction with reactive carbonyls produced by lipid peroxidation, but also by reactions with products of glycation. Lipofuscin thus should be considered as fluorescent pigment generated by modification of lipids and proteins through the action of lipid and carbohydrate reaction pathways. Schema of such processes generation of RPE lipofuscin from modified POS and fluorophore A2E is shown in Figure 6.

Our experiments indicate that fluorescent characteristics of the modified POS are essentially independent of the method of their modification. And various modifications of POS seem to have no or only a small influence on the spectral properties of obtaining lipofuscin.

Processes of fructozylation (glycation) and lipid peroxidation in POS cause fluorescence with the same maximum emission (445-450 nm) at an excitation wavelength of 365 nm. However, binding of the A2E fluorophore by modified POS led to a significant decrease of the original short wavelength emission maximum of modified POS. That also led to the appearance of a long-wave fluorescent peak, characteristic of the fluorescence profile of A2E. It also suggests that the fluorescence of lipofuscin is only slightly dependent on the nature of the fluorescent compounds arising from the modification of proteins and lipids. The fluorescence profile is mainly determined by the bisretinoid fluorophores present in lipofuscin granules.

Model lipofuscins prepared by fructozylation and lipid peroxidation contained approximately equal concentrations of fluorophore A2E and showed the same rate of superoxide photogeneration. Consequently, we hypothesize that the lipofuscin toxicity is independent from paths of protein and lipid modification. Instead, it mainly depends on the bisretinoid content.

ACKNOWLEDGMENTS

The authors would like to thank Professor Glickman RD from The University of Texas HSC at San Antonio for

the generous help and for much constructive criticism, helpful discussions and language editing.

COMMENTS

Background

Lipofuscinogenesis in the retinal pigment epithelium (RPE) cells is connected in many respects with formation of the modified proteins and the lipids incapable of degradation by lysosomal enzymes. Modification of proteins and lipids is carried out by their interaction with the active carbonyl compounds accumulated in reactions of lipid peroxidation and glycation. These two different ways of modification are used for preparing of model lipofuscin systems in this study.

Research frontiers

The authors examined the effect of different ways of protein-lipid modification of photoreceptor outer segments (POS) on the fluorescence characteristics and toxicity of model lipofuscins and compared them with properties of natural lipofuscin.

Innovations and breakthroughs

The results of this study are proposed that fluorescent characteristics and phototoxicity of lipofuscin granules depend only to an insignificant degree on the oxidative modification of proteins and lipids and generally are defined by bisretinoid fluorophores containing in them.

Applications

It is supposed that the fluorescence of RPE lipofuscin determines the fundus autofluorescence (FAF) *in vivo*. Monitoring FAF is noninvasive diagnostic method used in detection some retinal degenerative diseases such as recessive Stargardt disease, best macular dystrophy, and age-related macular degeneration. Preparation of model lipofuscins with predetermined fluorescent characteristics, defining by the relative content of the modified proteins and lipids, as well as the ratio of oxidized and reduced forms of fluorophores, is important for understanding the character of fluorescence ocular fundus and diagnostics associated pathologies. So the study of lipofuscin model systems may be an important factor for FAF interpretation.

Terminology

Lipofuscin is fluorescent pigment that accumulates in aging postmitotic tissues. In the eye lipofuscin is mainly accumulated in the RPE, being one of the key biomarkers of aging and oxidative stress. Lipofuscin also plays significant role in the development of retinal pathologies.

Peer-review

This is an interesting manuscript.

REFERENCES

1 **Jung T**, Bader N, Grune T. Lipofuscin: formation, distribution, and metabolic consequences. *Ann N Y Acad Sci* 2007; **1119**: 97-111 [PMID: 18056959 DOI: 10.1196/annals.1404.008]

2 **Boulton ME**. Studying melanin and lipofuscin in RPE cell culture models. *Exp Eye Res* 2014; **126**: 61-67 [PMID: 25152361 DOI: 10.1016/j.exer.2014.01.016]

3 **Sparrow JR**, Boulton M. RPE lipofuscin and its role in retinal pathobiology. *Exp Eye Res* 2005; **80**: 595-606 [PMID: 15862166 DOI: 10.1016/j.exer.2005.01.007]

4 **Sparrow JR**, Gregory-Roberts E, Yamamoto K, Blonska A, Ghosh SK, Ueda K, Zhou J. The bisretinoids of retinal pigment epithelium. *Prog Retin Eye Res* 2012; **31**: 121-135 [PMID: 22209824 DOI: 10.1016/j.preteyeres.2011.12.001]

5 **Sakai N**, Decatur J, Nakanishi K, Eldred GE. Ocular age pigment A2E: an unprecedented pyridinium bisretinoid. *J Am Chem Soc* 1996; **118**: 1559-1560 [DOI: 10.1021/ja953480g]

6 **Boulton M**, Dontsov A, Jarvis-Evans J, Ostrovsky M, Svistunenko D. Lipofuscin is a photoinducible free radical generator. *J Photochem Photobiol B* 1993; **19**: 201-204 [PMID: 8229462 DOI: 10.1016/1011-1344(93)87085-2]

7 **Kanofsky JR**, Sima PD, Richter C. Singlet-oxygen generation from A2E. *Photochem Photobiol* 2003; **77**: 235-242 [PMID: 12685649 DOI: 10.1562/0031-8655(2003)0770235SOGFA2.0.CO2]

8 **Rózanowska M**, Wessels J, Boulton M, Burke JM, Rodgers MA, Truscott TG, Sarna T. Blue light-induced singlet oxygen generation by retinal lipofuscin in non-polar media. *Free Radic Biol Med* 1998; **24**: 1107-1112 [PMID: 9626564 DOI: 10.1016/S0891-5849(97)00395-X]

9 **De S**, Sakmar TP. Interaction of A2E with model membranes. Implications to the pathogenesis of age-related macular degeneration. *J Gen Physiol* 2002; **120**: 147-157 [PMID: 12149277 DOI: 10.1085/jgp.20028566]

10 **Sokolov VS**, Sokolenko EA, Sokolov AV, Dontsov AE, Chizmadzhev YA, Ostrovsky MA. Interaction of pyridinium bis-retinoid (A2E) with bilayer lipid membranes. *J Photochem Photobiol B* 2007; **86**: 177-185 [PMID: 17070694]

11 **Dontsov AE**, Sakina NL, Ostrovsky MA. Comparative study of the dark and light-induced toxicity of lipofuscin granules from human retinal pigment epithelium and their chromophore A2E on the cardiolipin liposome model. *Russ Chem B* 2012; **61**: 442-448 [DOI: 10.1007/s11172-012-0061-2]

12 **Holz FG**, Schütt F, Kopitz J, Eldred GE, Kruse FE, Völcker HE, Cantz M. Inhibition of lysosomal degradative functions in RPE cells by a retinoid component of lipofuscin. *Invest Ophthalmol Vis Sci* 1999; **40**: 737-743 [PMID: 10067978]

13 **Höhn A**, Jung T, Grimm S, Catalgol B, Weber D, Grune T. Lipofuscin inhibits the proteasome by binding to surface motifs. *Free Radic Biol Med* 2011; **50**: 585-591 [PMID: 21167934 DOI: 10.1016/j.freeradbiomed.2010.12.011]

14 **Sitte N**, Huber M, Grune T, Ladhoff A, Doecke WD, Von Zglinicki T, Davies KJ. Proteasome inhibition by lipofuscin/ceroid during postmitotic aging of fibroblasts. *FASEB J* 2000; **14**: 1490-1498 [PMID: 10928983 DOI: 10.1096/fj.99-0843com]

15 **Finnemann SC**, Leung LW, Rodriguez-Boulan E. The lipofuscin component A2E selectively inhibits phagolysosomal degradation of photoreceptor phospholipid by the retinal pigment epithelium. *Proc Natl Acad Sci USA* 2002; **99**: 3842-3847 [PMID: 11904436 DOI: 10.1073/pnas.052025899]

16 **Powell SR**, Wang P, Divald A, Teichberg S, Haridas V, McCloskey TW, Davies KJ, Katzeff H. Aggregates of oxidized proteins (lipofuscin) induce apoptosis through proteasome inhibition and dysregulation of proapoptotic proteins. *Free Radic Biol Med* 2005; **38**: 1093-1101 [PMID: 15780767 DOI: 10.1016/j.freeradbiomed.2005.01.003]

17 **Suter M**, Remé C, Grimm C, Wenzel A, Jäättela M, Esser P, Kociok N, Leist M, Richter C. Age-related macular degeneration. The lipofusion component N-retinyl-N-retinylidene ethanolamine detaches proapoptotic proteins from mitochondria and induces apoptosis in mammalian retinal pigment epithelial cells. *J Biol Chem* 2000; **275**: 39625-39630 [PMID: 11006290 DOI: 10.1074/jbc.M007049200]

18 **Winkler BS**, Boulton ME, Gottsch JD, Sternberg P. Oxidative damage and age-related macular degeneration. *Mol Vis* 1999; **5**: 32 [PMID: 10562656]

19 **Schutt F**, Bergmann M, Holz FG, Kopitz J. Proteins modified by malondialdehyde, 4-hydroxynonenal, or advanced glycation end products in lipofuscin of human retinal pigment epithelium. *Invest Ophthalmol Vis Sci* 2003; **44**: 3663-3668 [PMID: 12882821 DOI: 10.1167/iovs.03-0172]

20 **Burcham PC**, Kuhan YT. Diminished susceptibility to proteolysis after protein modification by the lipid peroxidation product malondialdehyde: inhibitory role for crosslinked and noncrosslinked adducted proteins. *Arch Biochem Biophys* 1997; **340**: 331-337 [PMID: 9143338 DOI: 10.1006/abbi.1997.9903]

21 **Brownlee M**. Advanced protein glycosylation in diabetes and aging. *Annu Rev Med* 1995; **46**: 223-234 [PMID: 7598459 DOI: 10.1146/annurev.med.46.1.223]

22 **Yamagishi S**, Maeda S, Matsui T, Ueda S, Fukami K, Okuda S. Role of advanced glycation end products (AGEs) and oxidative stress in vascular complications in diabetes. *Biochim Biophys Acta* 2012; **1820**: 663-671 [PMID: 21440603 DOI: 10.1016/j.bbagen.2011.03.014]

23 **Glenn JV**, Stitt AW. The role of advanced glycation end products in retinal ageing and disease. *Biochim Biophys Acta* 2009; **1790**: 1109-1116 [PMID: 19409449 DOI: 10.1016/j.bbagen.2009.04.016]

24 **Yamada Y**, Ishibashi K, Ishibashi K, Bhutto IA, Tian J, Lutty GA, Handa JT. The expression of advanced glycation endproduct receptors in rpe cells associated with basal deposits in human maculas. *Exp Eye Res* 2006; **82**: 840-848 [PMID: 16364296 DOI: 10.1016/j.exer.2005.10.005]

25 **Glenn JV**, Mahaffy H, Wu K, Smith G, Nagai R, Simpson DA, Boulton ME, Stitt AW. Advanced glycation end product (AGE) accumulation on Bruch's membrane: links to age-related RPE dysfunction. *Invest Ophthalmol Vis Sci* 2009; **50**: 441-451 [PMID: 18676633 DOI: 10.1167/iovs.08-1724]

26 **Horie K**, Miyata T, Yasuda T, Takeda A, Yasuda Y, Maeda K, Sobue G, Kurokawa K. Immunohistochemical localization of advanced glycation end products, pentosidine, and carboxymethyllysine in lipofuscin pigments of Alzheimer's disease and aged neurons. *Biochem Biophys Res Commun* 1997; **236**: 327-332 [PMID: 9240434 DOI: 10.1006/bbrc.1997.6944]

27 **Delori FC**, Dorey CK, Staurenghi G, Arend O, Goger DG, Weiter JJ. In vivo fluorescence of the ocular fundus exhibits retinal pigment epithelium lipofuscin characteristics. *Invest Ophthalmol Vis Sci* 1995; **36**: 718-729 [PMID: 7890502]

28 **Delori FC**, Goger DG, Dorey CK. Age-related accumulation and spatial distribution of lipofuscin in RPE of normal subjects. *Invest Ophthalmol Vis Sci* 2001; **42**: 1855-1866 [PMID: 11431454]

29 Russian Federation law N 4180-I dated 22.12.1992. "On human organs or tissue transplantation" (with modifications and additions). Available from: URL: http://base.garant.ru/136366/

30 **Boulton M**, Marshall J. Repigmentation of human retinal pigment epithelial cells in vitro. *Exp Eye Res* 1985; **41**: 209-218 [PMID: 4065245 DOI: 10.1016/0014-4835(85)90026-0]

31 **McDowell JH**. Preparing rod outer segment membranes, regenerating rhodopsin, and determining rhodopsin concentration. In: Hargrave PA, editor. Methods in Neurosciences. *Academic Press NY* 1993; **15**: 123-130 [DOI: 10.1016/B978-0-12-185279-5.50013-3]

32 **Parish CA**, Hashimoto M, Nakanishi K, Dillon J, Sparrow J. Isolation and one-step preparation of A2E and iso-A2E, fluorophores from human retinal pigment epithelium. *Proc Natl Acad Sci USA* 1998; **95**: 14609-14613 [PMID: 9843937]

33 **Yakovleva MA**, Sakina NL, Kononikhin AS, Feldman TB, Nikolaev EN, Dontsov AE, Ostrovsky MA. Detection and study of the products of photooxidation of N-retinylidene-N-retinylethanolamine, the fluorophore of lipofuscin granules from retinal pigment epithelium of human donor eyes. *Doklady Biochem Biophys* 2006; **409**: 223-225 [DOI: 10.1134/S1607672906040089]

34 **Katz ML**, Gao CL, Rice LM. Formation of lipofuscin-like fluorophores by reaction of retinal with photoreceptor outer segments and liposomes. *Mech Ageing Dev* 1996; **92**: 159-174 [DOI: 10.1016/S0047-6374(96)01817-9]

35 **Buege JA**, Aust SD. Microsomal lipid peroxidation. *Methods Enzymology* 1978; **52**: 302-310 [DOI: 10.1016/S0076-6879(78)52032-6]

36 **McCord JM**, Fridovich I. Superoxide dismutase. An enzymic function for erythrocuprein (hemocuprein). *J Biol Chem* 1969; **244**: 6049-6055 [PMID: 5389100]

37 **Yamashita T**. Selective inhibition by the sulfhydryl reagent maleimide of zymosan particle phagocytosis by neutrophils. *FEBS Lett* 1982; **141**: 68-73 [PMID: 6123446 DOI: 10.1016/0014-5793(82)80018-5]

38 **Eldred GE**, Miller GV, Stark WS, Feeney-Burns L. Lipofuscin: resolution of discrepant fluorescence data. *Science* 1982; **216**: 757-759 [PMID: 7079738 DOI: 10.1126/science.7079738]

39 **Bilinska B**, Janikowska G, Zawada Z, Wylegala E, Dontsov A, Sakina N. Fluorescence spectra of lipofuscin isolated from human RPE cells. *Polish J Med Phys Eng* 2003; **9**: 121-135

40 **Ng KP**, Gugiu B, Renganathan K, Davies MW, Gu X, Crabb JS, Kim SR, Rózanowska MB, Bonilha VL, Rayborn ME, Salomon RG, Sparrow JR, Boulton ME, Hollyfield JG, Crabb JW. Retinal pigment epithelium lipofuscin proteomics. *Mol Cell Proteomics* 2008; **7**: 1397-1405 [PMID: 18436525 DOI: 10.1074/mcp.M700525-MCP200]

41 **Warburton S**, Southwick K, Hardman RM, Secrest AM, Grow RK, Xin H, Woolley AT, Burton GF, Thulin CD. Examining the proteins of functional retinal lipofuscin using proteomic analysis as a guide for understanding its origin. *Mol Vis* 2005; **11**: 1122-1134 [PMID: 16379024]

42 **Glickman RD**. Ultraviolet phototoxicity to the retina. *Eye Contact Lens* 2011; **37**: 196-205 [PMID: 21646980 DOI: 10.1097/ICL.0b013e31821e45a9]

43 **Wielgus AR**, Chignell CF, Ceger P, Roberts JE. Comparison of A2E cytotoxicity and phototoxicity with all-trans-retinal in human retinal pigment epithelial cells. *Photochem Photobiol* 2010; **86**: 781-791 [PMID: 20497365 DOI: 10.1111/j.1751-1097.2010.00750.x]

44 **Wielgus AR**, Roberts JE. Retinal photodamage by endogenous and xenobiotic agents. *Photochem Photobiol* 2012; **88**: 1320-1345 [PMID: 22582903 DOI: 10.1111/j.1751-1097.2012.01174.x]

45 **Baynes JW**. The role of AGEs in aging: causation or correlation. *Exp Gerontol* 2001; **36**: 1527-1537 [PMID: 11525875 DOI: 10.1016/S0531-5565(01)00138-3]

46 **Schalkwijk CG**, Stehouwer CD, van Hinsbergh VW. Fructose-mediated non-enzymatic glycation: sweet coupling or bad modification. *Diabetes Metab Res Rev* 2004; **20**: 369-382 [PMID: 15343583 DOI: 10.1002/dmrr.488]

47 **Huang SP**, Palla S, Ruzycki P, Varma RA, Harter T, Reddy GB, Petrash JM. Aldo-keto reductases in the eye. *J Ophthalmol* 2010; **2010**: 521204 [PMID: 20628518 DOI: 10.1155/2010/521204]

48 **Sato S**, Lin LR, Reddy VN, Kador PF. Aldose reductase in human retinal pigment epithelial cells. *Exp Eye Res* 1993; **57**: 235-241 [PMID: 8405190 DOI: 10.1006/exer.1993.1119]

49 **Vinores SA**, Campochiaro PA, Williams EH, May EE, Green WR, Sorenson RL. Aldose reductase expression in human diabetic retina and retinal pigment epithelium. *Diabetes* 1988; **37**: 1658-1664 [PMID: 3142801 DOI: 10.2337/diab.37.12.1658]

50 **Laroque D**, Inisan C, Berger C, Vouland E, Dufosse L, Guerard F. Kinetic study on the Maillard reaction. Consideration of sugar reactivity. *Food Chem* 2008; **111**: 1032-1042 [DOI: 10.1016/j.foodchem.2008.05.033]

51 **Tessier FJ**, Monnier VM, Sayre LM, Kornfield JA. Triosidines: novel Maillard reaction products and cross-links from the reaction of triose sugars with lysine and arginine residues. *Biochem J* 2003; **369**: 705-719 [PMID: 12379150 DOI: 10.1042/bj20020668]

52 **Asnaghi V**, Gerhardinger C, Hoehn T, Adeboje A, Lorenzi M. A role for the polyol pathway in the early neuroretinal apoptosis and glial changes induced by diabetes in the rat. *Diabetes* 2003; **52**: 506-511 [PMID: 12540628 DOI: 10.2337/diabetes.52.2.506]

P- Reviewer: Schoenhagen P, Tangvarasittichai S **S- Editor**: Ji FF
L- Editor: A **E- Editor**: Lu YJ

World Journal of Experimental Medicine

Submit a Manuscript: http://www.wjgnet.com/esps/
Help Desk: http://www.wjgnet.com/esps/helpdesk.aspx
DOI: 10.5493/wjem.v6.i4.72

World J Exp Med 2016 November 20; 6(4): 72-79
ISSN 2220-315X (online)

ORIGINAL ARTICLE

Basic Study

Morphogenesis of human embryonic stem cells into mature neurons under *in vitro* culture conditions

Geeta Shroff

Geeta Shroff, Nutech Mediworld, New Delhi 110016, India

Author contributions: Shroff G conceived and designed the study, and acquired, analyzed and interpreted the data. The author drafted the article and made critical revisions related to the intellectual content of the manuscript, and approved the final version of the article to be published.

Institutional review board statement: The study was reviewed and approved by the Institutional Review Board of Nutech Mediworld, New Delhi, India.

Informed consent statement: Not applicable.

Conflict-of-interest statement: The author declares no conflict of interest regarding the publication of this paper.

Data sharing statement: Our all publications are PubMed indexed and are available online (open access). We shall not be applying for membership of the Dryad Repository.

Manuscript source: Unsolicited manuscript

Correspondence to: Geeta Shroff, MBBS, Director, Nutech Mediworld, H-8, Green park extension, New Delhi 110016, India. geetashroff@hotmail.com
Telephone: +91-11-26180039
Fax: +91-11-26560089

Received: March 24, 2016
Peer-review started: March 24, 2016
First decision: May 16, 2016
Revised: May 25, 2016
Accepted: July 14, 2016

Article in press: July 16, 2016
Published online: November 20, 2016

Abstract

AIM

To describe the morphogenesis of different neuronal cells from the human embryonic stem cell (hESC) line, SCT-N, under *in vitro* culture conditions.

METHODS

The directed neuronal cell line was produced from a single, spare, pre-implantation stage fertilized ovum that was obtained during a natural *in vitro* fertilization process. The hESCs were cultured and maintained as per our proprietary in-house technology in a Good Manufacturing Practice, Good Laboratory Practice and Good Tissue Practice compliant laboratory. The cell line was derived and incubated in aerobic conditions. The cells were examined daily under a phase contrast microscope for their growth and differentiation.

RESULTS

Different neural progenitor cells (NPCs) and differentiating neurons were observed under the culture conditions. Multipotent NPCs differentiated into all three types of nervous system cells, *i.e.*, neurons, oligodendrocytes and astrocytes. Small projections resembling neurites or dendrites, and protrusion coming out of the cells, were observed. Differentiating cells were observed at day 18 to 20. The differentiating neurons, neuronal bodies, axons, and neuronal tissue were observed on day 21 and day 30 of the culture. On day 25 and day 30, prominent neurons, axons and neuronal tissue were observed under phase contrast microscopy. 4′, 6-diamidino-2-phenylindole staining also indicated the pattern of differentiating neurons, axonal structure and neuronal tissue.

CONCLUSION

This study describes the generation of different ne-

uronal cells from an hESC line derived from biopsy of blastomeres at the two-cell cleavage stage from a discarded embryo.

Key words: Human embryonic stem cells; Multipotency; Neural differentiation; Neural progenitor cells; *In-vitro* fertilization

Core tip: Human embryonic stem cells (hESCs) have the capability to regenerate and differentiate into a wide variety of cells. In the present study, we described the morphogenesis of different neuronal cells from an hESC line under *in vitro* culture conditions. The blastomeres were at the two-cell cleavage stage and were taken from a discarded embryo during an *in vitro* fertilization process. We showed that neuronal axons and tissues were generated by the joining of multiple cells that communicate and transfer signals to each other, thereby forming neuronal cells and tissue.

Shroff G. Morphogenesis of human embryonic stem cells into mature neurons under *in vitro* culture conditions. *World J Exp Med* 2016; 6(4): 72-79 Available from: URL: http://www.wjgnet.com/2220-315X/full/v6/i4/72.htm DOI: http://dx.doi.org/10.5493/wjem.v6.i4.72

INTRODUCTION

Human embryonic stem cells (hESCs) offer an unlimited source of human cells[1]. hESCs have the capability to renew and differentiate into all cell types. Differentiation may occur at all development stages upon exposure to the appropriate signals. These signals act in a hierarchical manner that regulates the development of the embryo, which induces the hESCs to differentiate into specific cell types of the three germ layers[2,3].

The pluripotent characteristic of hESCs is considered as a "double-edged sword". The determination of how to direct hESCs to a specific progenitor cell type is a major challenge[1]. hESCs are a renewable source of neural cells[4]. Different protocols are used to direct the neural differentiation of hESCs; however, across all culture systems, common signals and stages of differentiation are observed. The three main stages of hESCs' neural differentiation are neural induction, neural stem/progenitor expansion, and neuronal and glial differentiation. These stages may further be subdivided into multiple events to progress a stem cell through its different progenitor stages[1].

The human neuronal system is ectodermal in origin and contains multipotent stem cells, *i.e.*, neuronal stem cells or neural progenitor cells (NPCs), which give rise to the different cells of the nervous system. Multipotency, the ability to differentiate into different types of neuronal cells, *viz.* neurons, astrocytes and oligodendrocytes, is the key characteristics of NPCs[5,6]. hESCs can be differentiated into NPCs that exhibit a broad cellular developmental and lineage spectrum[7,8]. According to Wu *et al*[9], *in vitro* differentiation of hESCs and *in vivo* embryonic formation of the neuroectoderm share some similarities.

The present study describes the generation of different neuronal cells from an hESC line (SCT-N) produced from biopsied blastomeres at the two-celled cleavage stage from a discarded embryo during an *in vitro* fertilization (IVF) process. These cells use defined animal free conditions during derivation and long-term culture, which make them suitable for clinical cell therapy. We showed that neuronal axons and tissues were not generated from single cell differentiation, but were produced by the joining of multiple cells that communicate and transfer signals to each other, thereby forming neuron tissue.

MATERIALS AND METHODS

Ethics statement

The study protocol was approved by an independent Institutional Ethics Committee (IEC) of Nutech Mediworld. The institutional committee for stem cell research and therapy of Nutech Mediworld, New Delhi, India reported the study to the National Apex Committee for Stem Cell Research and Therapy (NAC-SCRT). The study was conducted according to the Declaration of Helsinki[3].

Origin of the cell line

The directed cell line (neuronal) was obtained from a single, spare, pre-implantation stage fertilized ovum that was obtained during a natural IVF process. The donor gave her consent.

The hESCs were cultured and maintained according to our proprietary in-house technology (United States Granted Patent No US 8592, 208, 52) in a Good Manufacturing Practice (GMP), Good Laboratory Practice (GLP) and Good Tissue Practice (GTP) compliant laboratory. The cell lines were chromosomally stable and free from any animal product. The detailed cell culture and differentiation techniques were described in our previous paper[10].

Cell culture and derivation

The embryo was suspended in Roswell Park Memorial Institute (RPMI) medium and broken mechanically. Human beta-chorionic gonadotropin (β-hCG) and progestin were added and the cells were incubated in a CO_2 water-jacketed incubator for 24 h in aerobic conditions. The cell suspension was then re-incubated in the same incubator after adding Dulbecco's Modified Eagle's Medium (DMEM, Himedia Labs, Mumbai, India) under anaerobic conditions. The details of cell culture and derivation are explained in our previous paper[10].

For this experiment, the above cell line was taken and re-incubated in aerobic conditions after the addition of DMEM. The cells were examined daily for the growth

and differentiation of the neural tissue.

Sample collection and characterization

Syringes of frozen cells containing 2.5 to 3.5 million cells per milliliter were thawed and raised to body temperature. After this slow thawing process, the cells were characterized for their expression of different markers[11] using reverse transcription polymerase chain reaction RT-PCR on a Bio-Rad T100 (Bio-Rad Laboratories Inc., Hercules, CA, United States) ,immunofluorescence using a Nikon Ellipse E200 (Nikon corporation, Minato-ku, Tokyo, Japan) and fluorescence-activated cell sorting (FACS).

Sterility tests

A quality check for the integrity, viability and microbial contamination was performed for the stored cell batches and the cultured cells obtained from the GLP laboratory.

Phase contrast/confocal microcopy

To investigate the differentiation of hESCs into different NPCs and neuronal tissue, hESCs were cultured for one month (day 0 of inoculation to day 30 of the culture). The cells were observed for differentiation at different days under a phase contrast microscope (Nikon Ellipse E200), which was used as the major instrument to determine neuronal differentiation.

4', 6-diamidino-2-phenylindole (DAPI) staining of cultured cells

To determine the presence of nuclei and chromatin materials, hESCs were stained with DAPI. The cells were incubated in a DAPI solution at a concentration of 0.1-1 μg/mL for 5 min. DAPI stained cells were mounted in ProLong® Gold Antifade (Life technologies, OR, United States) and were evaluated under a fluorescence microscope.

Neuronal Nuclei (NeuN) staining

The expression of the *NeuN* gene was examined in cells cultured for different days (0-30 d). The cultured cells were reacted with an anti-NeuN antibody. The staining was performed at day 4, 8, 16, 22 and 30 of culture.

Immunofluorescence

Cells (1×10^6) were adhered on a cover slide coated with poly-L-lysine, followed by washing in PBS and fixing for 10-20 min in 4% paraformaldehyde (PFA) at room temperature. The cells were permeabilized in Triton-X (0.25%) for 20 min. BSA (2%) and donkey (5%) serum were used to block the PBS washed cells for 2 h.

The treated cells were incubated at 37 ℃ with a primary antibody against NeuN (1:100, Neuromics) and then with the secondary antibody Alexa fluor© 488 donkey (SC2044) anti-mouse IgG (Invitrogen, Life technology, 557782) for 1 h and 30 min respectively. The cells were counterstained with 0.1-1 μg/mL DAPI for 5 min, mounted in ProLong® Gold Antifade (Life technologies, OR, United States) and evaluated under a fluorescence microscope (Nikkon Micro E200).

RESULTS

Sterility tests

All the cell batches and the cultured cells were found to be viable and sterile. No microbial contamination was observed.

Differentiation of neuronal progenitor cells into neurons, oligodendrocytes and astrocytes

Different NPCs and differentiating neurons were observed in the hESCs culture. Multipotent NPCs differentiated into all three types of cells of the nervous system, *i.e.*, neurons, oligodendrocytes and astrocytes, as observed under a phase contrast microscope (Figure 1).

Determination of morphological differentiation of hESCs into neurons and neuronal tissue by phase contrast microscopy

The hESCs were cultured for 30 d and observed at regular interval under a phase contrast microscope. Low cell numbers were observed just after inoculation; however, after 24-48 h of culture, the cell number increased and the cells started to clump together. Further culture led to an increase in cell size and the generation of NPCs (Figure 2). From 6-8 d of culture, we observed increased numbers of NPCs, while some of the cells showed the first signs of differentiation.

We observed small projections, such as those on neurites or dendrites, and protrusions coming out of the cells. Significant differentiation of the cells was observed at 18-20 d of culture.

Differentiating neurons, neuronal bodies, axons and neuronal tissue were observed on day 21 and day 30 of culture. On day 25 and day 30, prominent neurons, axons and neuronal tissue were observed under phase contrast microscopy.

DAPI staining of differentiating neuronal cells

Further validation of the cells' morphology, differentiation pattern, presence of chromatin material and presence of tissue structure in culture were examined by DAPI (nuclear staining). The DAPI staining confirmed the presence of nuclei inside the cells. DAPI staining was more prominent in smaller cells compared with larger cells, probably because the larger cells were less permeable to DAPI compared with smaller cells (Figure 3).

DAPI staining also indicated the pattern of differentiating neurons, axonal structure and neuronal tissue.

Expression profile of NeuN, an intracellular neuronal marker, in hESCs in culture, as determined by immunofluorescence and confocal microscopy

NeuN staining of cells was observed on day 4, 8, 16, 22 and 30 of culture. We observed the staining of the cells from day 4 of culture, which continued on day 8, 16, 22 and 30 of culture. Tissue staining was observed on day

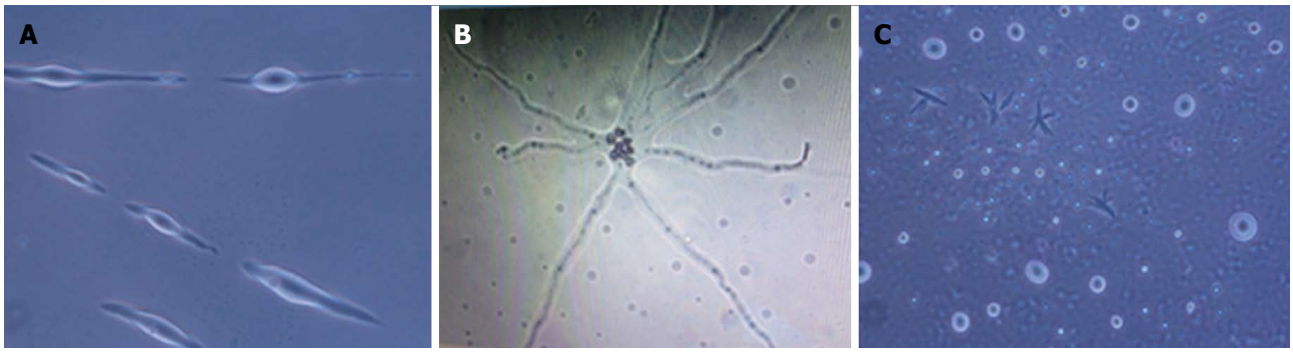

Figure 1 Differentiation of neuronal progenitor cells into neuronal cells, oligodendrocytes and astrocytes under *in vitro* culture conditions. A: Neuron; B: Oligodendrocytes; C: Astrocytes.

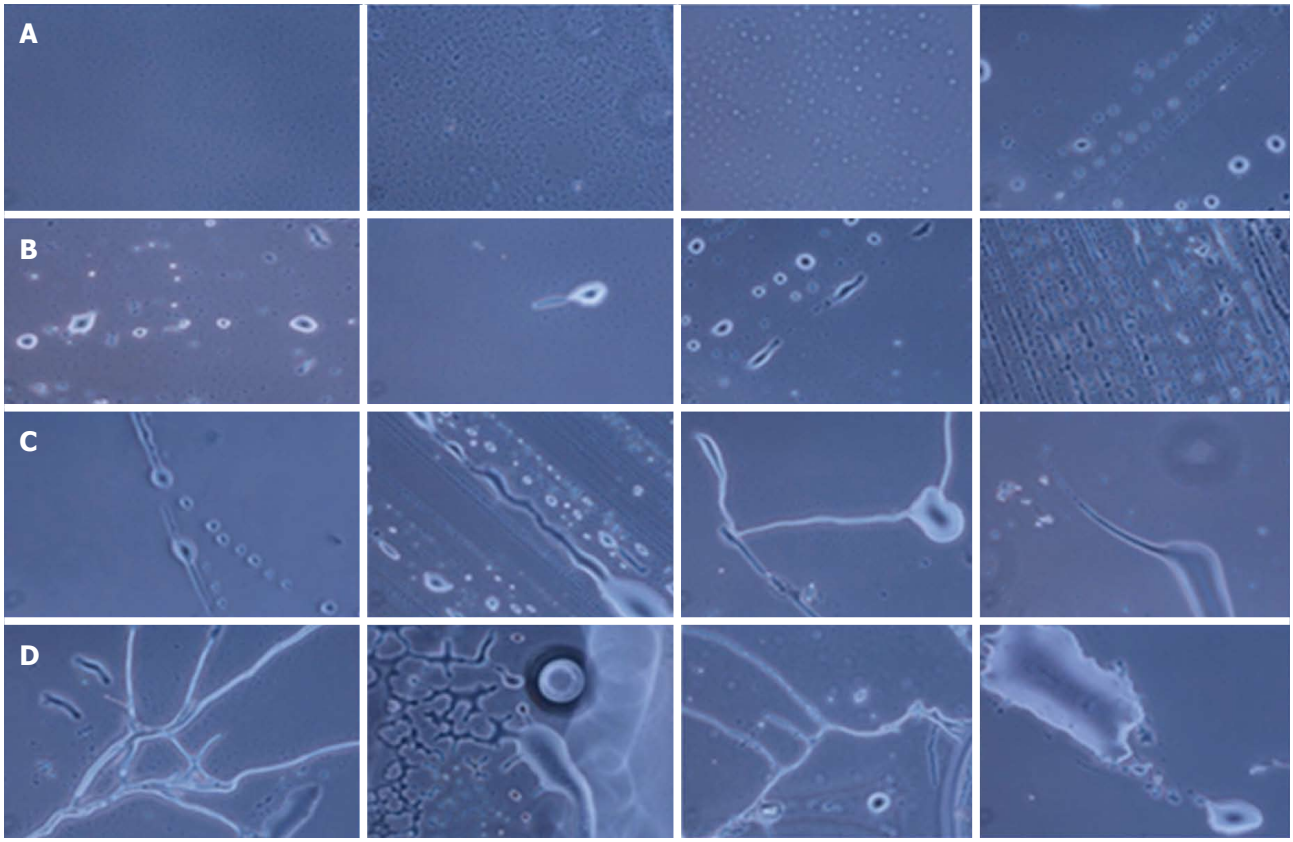

Figure 2 Phase contrast images of neuronal cells and tissues at different days of culture. A: Day 0: Small stem cells; B: Day 5: Differentiating neurons; C: Day 16-18: Small protrusions, neuritis structure and end-joining of neurons; D: Day 30: Complete neurons and neuronal tissue.

16 onwards (Figure 4).

Determination of the mechanism of neuronal axons and tissue formation under in vitro culture conditions

During the formation of neurons, neuronal axons and neuronal tissue, the NPCs were first arranged in a line and then differentiated into neuronal cells with single or multiple projections. Furthermore, these projections joined the progenitor cells and increased in size, giving rise to small single protrusions. This protrusion increased in length and then joined to another cell's projection. The joining of one cell projection to another might either be direct or *via* joining to other progenitor cells. In this way, these cells formed a chain and their cytoplasmic materials fused together to form neuronal axons (Figure 5).

Likewise, for the formation of neuronal tissue, the cells were first arranged in a line and then their projections joined together to form a network-like structure. Further growth and development of these joined cells in a network led to the development of the neuronal tissue. We also observed branching of neurons by the joining of single cell progenitor cells.

Under our culture condition, we observed that during differentiation of NPCs, all the cells do not commit towards differentiation at the same time. We hypothesized that among these cells, if one cell commits to differentiation,

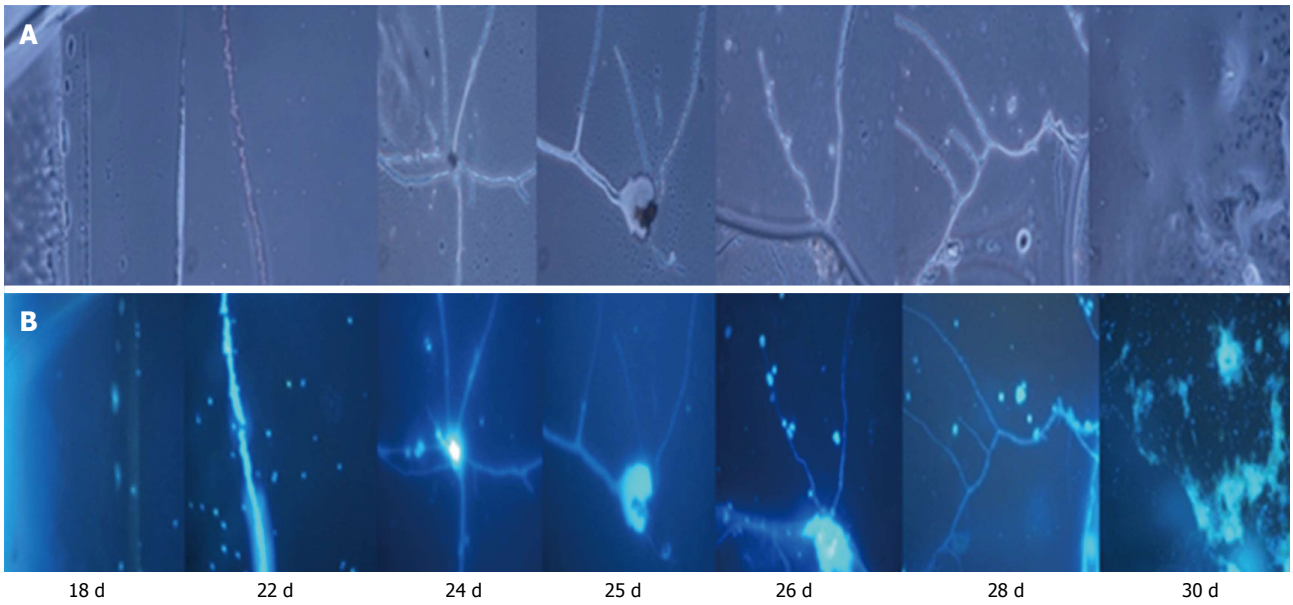

Figure 3 4', 6-diamidino-2-phenylindole staining of neuronal specific cells and tissues under *in vitro* culture condition. A: Cells viewed under a phase contrast microscope; B: 4'6-diamidino-2-phenylindole stained cells.

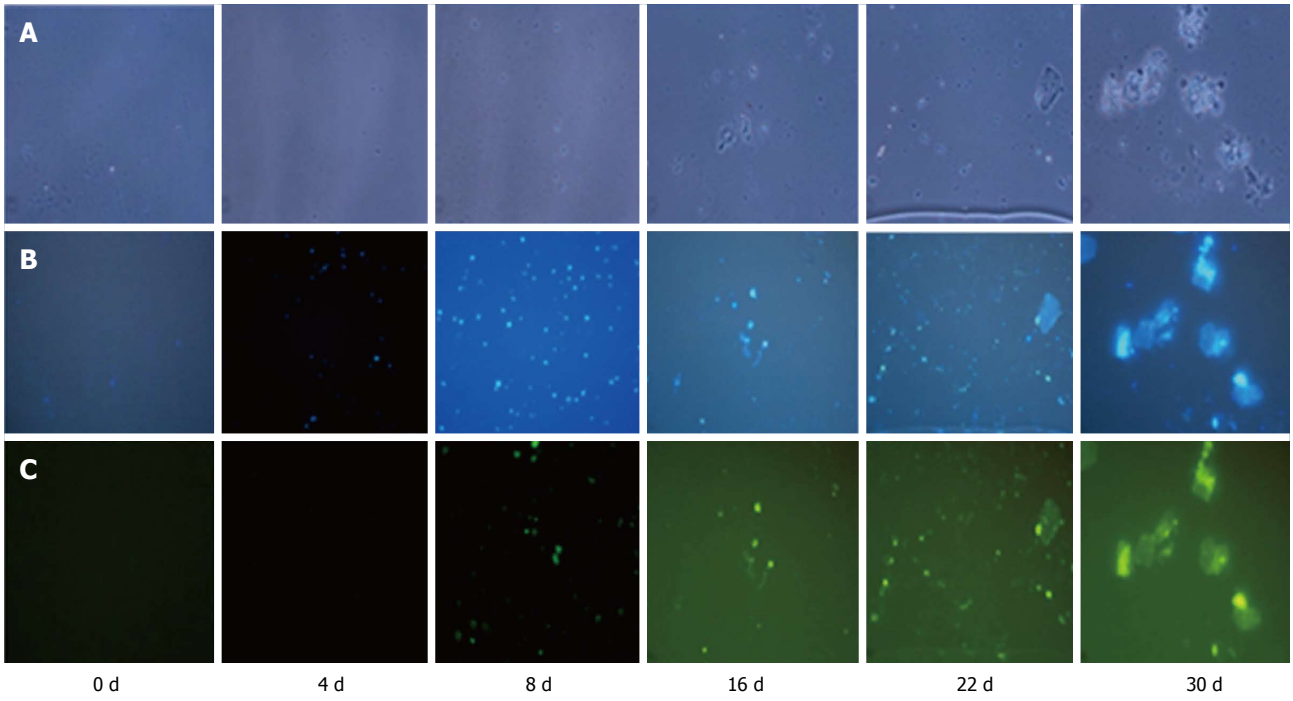

Figure 4 Differentiation of human embryonic stem cells into neuronal specific cells and tissues under *in vitro* culture conditions. A: Cells viewed under a phase contrast microscope; B: 4', 6-diamidino-2-phenylindole stained cells; C: Green (*NeuN*) stained cells.

other surrounding cells will assist these progenitor cells for their growth, development and differentiation.

In this *in vitro* culture, we could observe single neuronal cell differentiation and the spread of a tissue-like structure. By joining together, these cells communicate and transfer signals to each other.

DISCUSSION

In the present study, we determined the ability of hESCs to differentiate into several neural cells and tissue. We showed the mechanism of division and differentiation of single NPCs into neurons, axons and neuronal tissue. Our results indicated that differentiation of hESCs towards lineage specific cells or tissue involves the generation of lineage-specific progenitors from hESCs that then undergo differentiation.

The pluripotent nature of hESCs allow them to generate the neuronal and glial cells found in neural tissue[5]. To direct and understand the differentiation process of hESCs into

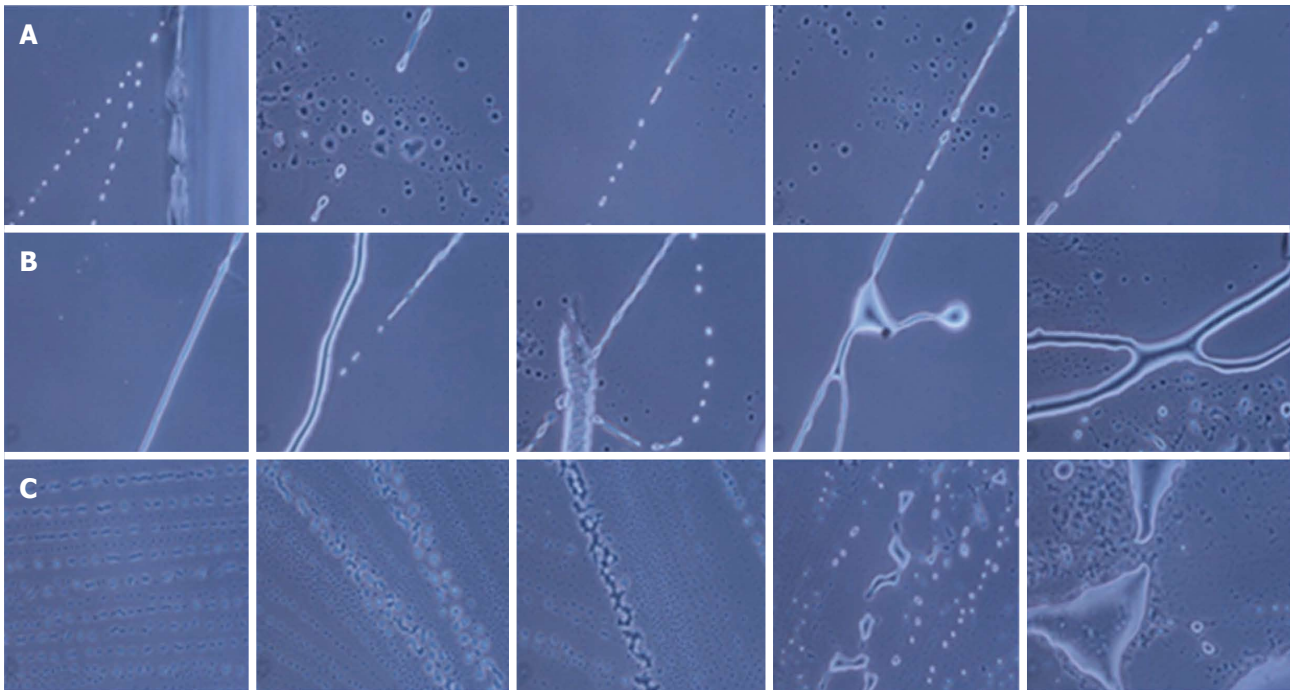

Figure 5 Mechanism of differentiation of human embryonic stem cells into neurons and axons formation under *in vitro* culture conditions. A: Day 5: Neural progenitor cells increased in size, arranged in a line and then joined together through small protrusions; B: Day 16-18: Cytoplasmic material mixed together to form long axonal structure; C: Day 30: Formation of neuronal tissue.

neuronal lineages, we cultured the cells in normal culture media, which was free from feeder layers and animal product. A unique feature of this culture media was that it did not contain any supplements. Under these culture conditions, the differentiation pattern of the stem cells was similar to the accepted model of the adult human and mouse nervous system differentiation process[12,13]. Ying *et al*[14] cultured embryonic stem cells (ESCs) in defined serum-free and feeder-free conditions, in the absence of bone morphogenetic proteins (BMP) signals, which resulted in efficient neural commitment and differentiation. Our results indicated that our unique culture conditions allow the lineage specific differentiation of neuronal cells without adding supplements.

In our study, hESCs generated NPCs that were capable of differentiating into neural cells and tissue. Microscopy revealed three types of nervous system cells, *i.e*., neurons, oligodendrocytes and astrocytes. A previous study by Rubinoff *et al*[4] reported similar results: The proliferating progenitors generated from hESCs were able to differentiate into astrocytes, oligodendrocytes and neurons. Similarly, Zhang *et al*[15] demonstrated that hESCs-derived neural precursors generated all three types of neuronal cells *in vitro*.

After establishing the differentiation of hESCs in our culture conditions, we studied how hESCs were differentiated into neurons and neuronal tissue and the time course of differentiation. The differentiation stages of hESCs were followed at different days (0 day to 30th day). The cells started growing and were arranged in a line. Arranging of the cells in a line was identified as a characteristic of neuronal differentiation in our culture conditions. After culturing hESCs for a week, small projections started to come out of the cells. The multipotent NPCs underwent asymmetrical cell division, which gave rise to smaller, undifferentiated multipotent stem cells and differentiated neuron cells. Hence, our results confirm the potential of hESCs to differentiate into neural cells. These results are consistent with previous studies[16]. In a study by Zhang *et al*[15], hESCs differentiated to form neural tube-like rosette structures by day 7 of cell culture in a defined medium. Rubinoff *et al*[4] cultured hESCs for 3 to 4 wk to induce differentiation and derivation of NPCs. Early differentiation started after a week of culture, as indicated by changes in the cell morphology observed at the center of the colonies under phase contrast microscopy. Differentiation accelerated during next two weeks. Abranches *et al*[12] cultured ESCs for several days and observed that the cells developed very long cellular projections similar to those of radial glia, which then differentiated into all three neural lineages.

Differentiation of hESCs towards neuronal lineages leads to expression of neuronal-specific markers. Therefore, after establishing the differentiation of neurons and neuronal tissue in our culture conditions, we also confirmed the expression of neuronal system specific markers by immunofluorescence microscopy. *NeuN* is a specific marker that is expressed in neuronal differentiated cells and tissues[17]. Expression of this neuron-specific nuclear protein is a reliable marker of proliferative capacity that might indicate the physiological status of a post mitotic neuron[18]. In our previous study, we observed the expression of neuronal lineage-specific markers like nestin (neuronal progenital cells, NPCs) and *NeuN* (neuronal

marker of differentiated cells) in hESCs at the mRNA level[10]. On the 8th day of culture, we observed staining of smaller cells with the anti-NeuN antibody, which indicated that the cells might be entering differentiating mode. On day 30 of culture, we observed the staining of differentiated cells and differentiated tissue, which indicated that the later stage of the culture contained both differentiating cells and tissues. The spontaneous expression of neural markers may be considered as an evidence of the hESCs' differentiation towards neural lineages.

We also determined the mechanism of neuronal axons and tissue formation under *in vitro* culture conditions. Most of the studies on neurons and neuronal tissues differentiation have been done with either stem cells isolated from the pluripotent blastocyst stage or multipotent adult stem cells. These cells were found to account for the morphology and antigenic properties of neurons and astrocytes after their division and differentiation into neurons and astrocytes, respectively[19,20]. Reynolds *et al*[20] demonstrated the induced *in vitro* proliferation of striatum-isolated cells *via* epidermal growth factor. As far as we know, this is the first study to explain the mechanism of neuron network formation, axon formation and neuronal tissue differentiation of hESCs. Based on the principle that a brain-like structure can emerge as a self-organizing cytoarchitecture from stem cells *in vitro*[19], we were able to show the mechanism of differentiation, extension of axons, cell joining and tissue differentiation from totipotent hESCs during *in vitro* culture. In our culture conditions, the pattern of aligning in a row of hESCs was found to be a characteristic feature of neuronal differentiating cells. We also observed that all the cells do not differentiate simultaneously, rather multiple single cells first align together and then join together through small protrusions, thereby forming neuronal cells, axon and tissue.

This study provided a system for generation of NPCs from hESCs. Moreover, the resulting NPCs from hESCs could serve as an expandable source for neuron production, which could be applied for many purposes, such as the treatment of neurodegenerative diseases. Recently, clinical trials using hESC derivatives to treat several neurodegenerative diseases have been approved, which led to the derivation of specific cell types from hESCs[6]. The development of neuronal tissue differentiation protocols will expand the application of hESCs-derived NPCs to neurological diseases. The stem cells used in our study have been injected into patients suffering from various neurodegenerative diseases such as cerebral palsy, spinal cord injury and Friedreich's ataxia and have shown successful results[11,21-23].

To understand how to manipulate stem cells, and to restore and repair neural circuitry, it is important to identify the signals and mechanisms involved at each of these stages[1]. In view of the importance of understanding self-renewal and differentiation of hESCs at the transcriptional level, further studies are needed. This study will have a significant impact on the emerging field of regenerative medicine.

ACKNOWLEDGMENTS

The author acknowledges Knowledge Isotopes Pvt. Ltd. (www.knowledgeisotopes.com) for their assistance with writing the paper.

COMMENTS

Background

Human embryonic stem cells (hESCs) offer an unlimited source of cells. They have the capability to renew and differentiate into all cell types. Differentiation may occur at all development stages upon exposure to appropriate signals. These signals act in a hierarchical manner that regulates the development of the embryo, which induces the hESCs to differentiate into specific cell types of three germ layers.

Research frontiers

The study describes the generation of different neuronal cells from the cell line SCT-N produced using hESCs from biopsy of blastomeres at the two-celled cleavage stage from a discarded embryo during an *in vitro* fertilization process.

Innovations and breakthroughs

The hESC line uses defined animal free conditions during its derivation and long-term culture, which makes it suitable for clinical cell therapy. The author showed that neuronal axons and tissues were not generated from single cell differentiation but by the joining of multiple cells that communicate and transfer signals to each other, thereby forming neuronal tissue.

Applications

The study provided a system to generate neural progenitor cells (NPCs) from hESCs. Moreover, the resulting NPCs could serve as an expandable source for neurons production, which could be applied for many purposes, such as the treatment of neurodegenerative diseases.

Terminology

NPCs are multipotent, self-renewable cells that are responsible for forming the main phenotype of the nervous system.

Peer-review

The paper "Morphogenesis of human embryonic stem cells into mature neurons under *in vitro* culture conditions" by Shroff, describes the differentiation of hESCs into neurons. It is a rapidly growing field of translational research that combines high expectations and safety concerns. Maintaining hESCs in defined conditions under strict GMP regulations is a very important part of the research, together with detailed step-by-step descriptions of differentiating cells and their characterization.

REFERENCES

1 **Denham M**, Dottori M. Signals involved in neural differentiation of human embryonic stem cells. *Neurosignals* 2009; **17**: 234-241 [PMID: 19816060 DOI: 10.1159/000231890]

2 **Hay DC**, Zhao D, Fletcher J, Hewitt ZA, McLean D, Urruticoechea-Uriguen A, Black JR, Elcombe C, Ross JA, Wolf R, Cui W. Efficient differentiation of hepatocytes from human embryonic stem cells exhibiting markers recapitulating liver development in vivo. *Stem Cells* 2008; **26**: 894-902 [PMID: 18238852 DOI: 10.1634/stemcells. 2007-0718]

3 **Thomson JA**, Itskovitz-Eldor J, Shapiro SS, Waknitz MA, Swiergiel JJ, Marshall VS, Jones JM. Embryonic stem cell lines derived from human blastocysts. *Science* 1998; **282**: 1145-1147 [PMID: 9804556 DOI: 10.1126/science.282.5391.1145]

4 **Reubinoff BE**, Itsykson P, Turetsky T, Pera MF, Reinhartz E, Itzik

A, Ben-Hur T. Neural progenitors from human embryonic stem cells. *Nat Biotechnol* 2001; **19**: 1134-1140 [PMID: 11731782 DOI: 10.1038/nbt1201-1134]
5 **Willerth SM**. Neural tissue engineering using embryonic and induced pluripotent stem cells. *Stem Cell Res Ther* 2011; **2**: 17 [PMID: 21539726 DOI: 10.1186/scrt58]
6 **Noisa P**, Raivio T, Cui W. Neural Progenitor Cells Derived from Human Embryonic Stem Cells as an Origin of Dopaminergic Neurons. *Stem Cells Int* 2015; **2015**: 647437 [PMID: 26064138 DOI: 10.1155/2015/647437]
7 **Chambers SM**, Fasano CA, Papapetrou EP, Tomishima M, Sadelain M, Studer L. Highly efficient neural conversion of human ES and iPS cells by dual inhibition of SMAD signaling. *Nat Biotechnol* 2009; **27**: 275-280 [PMID: 19252484 DOI: 10.1038/nbt.1529]
8 **Gerrard L**, Rodgers L, Cui W. Differentiation of human embryonic stem cells to neural lineages in adherent culture by blocking bone morphogenetic protein signaling. *Stem Cells* 2005; **23**: 1234-1241 [PMID: 16002783 DOI: 10.1634/stemcells. 2005-0110]
9 **Wu JQ**, Habegger L, Noisa P, Szekely A, Qiu C, Hutchison S, Raha D, Egholm M, Lin H, Weissman S, Cui W, Gerstein M, Snyder M. Dynamic transcriptomes during neural differentiation of human embryonic stem cells revealed by short, long, and paired-end sequencing. *Proc Natl Acad Sci USA* 2010; **107**: 5254-5259 [PMID: 20194744 DOI: 10.1073/pnas.0914114107]
10 **Shroff G**. Establishment and characterization of a neuronal cell line derived from a 2-cell stage human embryo: clinically tested cell-based therapy for neurological disorders. *Int J Recent Sci Res* 2015; **6**: 3730-3738
11 **Shroff G**, Gupta A, Barthakur JK. Therapeutic potential of human embryonic stem cell transplantation in patients with cerebral palsy. *J Transl Med* 2014; **12**: 318 [PMID: 25496119 DOI: 10.1186/s12967-014-0318-7]
12 **Abranches E**, Silva M, Pradier L, Schulz H, Hummel O, Henrique D, Bekman E. Neural differentiation of embryonic stem cells in vitro: a road map to neurogenesis in the embryo. *PLoS One* 2009; **4**: e6286 [PMID: 19621087 DOI: 10.1371/journal.pone.0006286]
13 **Oikari LE**, Griffiths LR, Haupt LM. The current state of play in human neural stem cell models: what we have learnt from the rodent. *OA Stem Cells* 2014; **2**: 7
14 **Ying QL**, Stavridis M, Griffiths D, Li M, Smith A. Conversion of embryonic stem cells into neuroectodermal precursors in adherent monoculture. *Nat Biotechnol* 2003; **21**: 183-186 [PMID: 12524553 DOI: 10.1038/nbt780]
15 **Zhang SC**, Wernig M, Duncan ID, Brüstle O, Thomson JA. In vitro differentiation of transplantable neural precursors from human embryonic stem cells. *Nat Biotechnol* 2001; **19**: 1129-1133 [PMID: 11731781 DOI: 10.1038/nbt1201-1129]
16 **Ahmad R**, Wolber W, Eckardt S, Koch P, Schmitt J, Semechkin R, Geis C, Heckmann M, Brüstle O, McLaughlin JK, Sirén AL, Müller AM. Functional neuronal cells generated by human parthenogenetic stem cells. *PLoS One* 2012; **7**: e42800 [PMID: 22880113 DOI: 10.1371/journal.pone.0042800]
17 **Mullen RJ**, Buck CR, Smith AM. NeuN, a neuronal specific nuclear protein in vertebrates. *Development* 1992; **116**: 201-211 [PMID: 1483388]
18 **Weyer A**, Schilling K. Developmental and cell type-specific expression of the neuronal marker NeuN in the murine cerebellum. *J Neurosci Res* 2003; **73**: 400-409 [PMID: 12868073 DOI: 10.1002/jnr.10655]
19 **Gaspard N**, Vanderhaeghen P. Mechanisms of neural specification from embryonic stem cells. *Curr Opin Neurobiol* 2010; **20**: 37-43 [PMID: 20080043 DOI: 10.1016/j.conb.2009.12.001]
20 **Reynolds BA**, Weiss S. Generation of neurons and astrocytes from isolated cells of the adult mammalian central nervous system. *Science* 1992; **255**: 1707-1710 [PMID: 1553558]
21 **Shroff G**. A novel approach of human embryonic stem cells therapy in treatment of Friedreich's ataxia. *Int J Case Rep Images* 2015; **6**: 261-266 [DOI: 10.5348/ijcri-201503-CS-10054]
22 **Shroff G**, Das L. Human embryonic stem cell therapy in cerebral palsy children with cortical visual impairment: a case series of 40 patients. *J Cell Sci Ther* 2014; **5**: 189 [DOI: 10.4172/2157-7013.1000189]
23 **Shroff G**, Gupta R. Human embryonic stem cells in the treatment of patients with spinal cord injury. *Ann Neurosci* 2015; **22**: 208-216 [PMID: 26526627 DOI: 10.5214/ans.0972.7531.220404]

P- Reviewer: Bártová E, Kiselev SL, Tanabe S **S- Editor**: Qiu S
L- Editor: A **E- Editor**: Lu YJ

Published by **Baishideng Publishing Group Inc**
8226 Regency Drive, Pleasanton, CA 94588, USA
Telephone: +1-925-223-8242
Fax: +1-925-223-8243
E-mail: bpgoffice@wjgnet.com
Help Desk: http://www.wjgnet.com/esps/helpdesk.aspx
http://www.wjgnet.com